

Modeling the Hazard Function with Non-linear Systems in Dynamical Survival Analysis

Dananjani Liyanage *

Mahmudul Bari Hridoy[†]

Fahad Mostafa^{‡§}

Abstract

Hazard functions play a central role in survival analysis, offering insight into the underlying risk dynamics of time-to-event data, with broad applications in medicine, epidemiology, and related fields. First-order ordinary differential equation (ODE) formulations of the hazard function have been explored as extensions beyond classical parametric models. However, such approaches typically produce monotonic hazard patterns, limiting their ability to represent oscillatory behavior, nonlinear damping, or coupled growth–decay dynamics. We propose a new statistical framework for modeling and simulating hazard functions governed by higher-order ODEs, allowing risk to depend on both its current level, its rate of change, and time. This class of models captures complex time-dependent risk behaviors relevant to survival analysis and reliability studies. We develop a simulation procedure by reformulating the higher-order ODE as a system of nonlinear first-order equations solved numerically, with failure times generated via cumulative hazard inversion. Likelihood-based inference under right censoring is also developed, and moment generating function analysis is used to characterize tail behavior. The proposed framework is evaluated through simulation studies and illustrated using real-world survival data, where oscillatory hazard dynamics capture temporal risk patterns beyond standard monotone models.

Keywords Survival Analysis, Non-linear ODEs, Inference, Dynamical Systems

AMS Classification 62N99; 62P10; 62P99; 62P35

1 Introduction

Survival Analysis is a statistical framework for modeling and analyzing time-to-event data, focusing on the timing of specific events of interest, such as death, system failure, disease progression, or recovery. Classical methods address practical complications such as right censoring and truncation, which arise when complete event information is not available. The core components include the survival function, which estimates the probability of surviving beyond a given time, and the hazard function, which characterizes the instantaneous risk of event occurrence. In particular, the hazard function offers a dynamic perspective on risk evolution over time, which makes it especially suitable for modeling through differential equations.

The historical roots of survival analysis trace back to early life tables, beginning with John Graunt’s pioneering work in 1662 and further advanced by Edmund Halley’s probabilistic life table

*Department of Mathematics and Statistics, University of Minnesota Duluth, dmadiwal@d.umn.edu

[†]Department of Mathematics, Virginia Tech, barihridoy@vt.edu

[‡]School of Mathematical and Natural Sciences, and Julie Ann Wrigley Global Futures Laboratory, Arizona State University, fahad.mostafa@asu.edu

[§]Corresponding author’s email: fahad.mostafa@asu.edu/fahadraj.du@gmail.com

in 1693 [1]. Traditional survival models typically employ parametric approaches, assuming that survival times follow predefined probability distributions such as Weibull, Exponential, or Log-Normal [2]. These methods impose rigid functional forms on survival and hazard functions, leading to limitations in capturing complex survival dynamics [2, 3]. While effective for hazard functions with constant or monotonic rates, parametric models struggle with time-varying covariates, feedback mechanisms, and model misspecification [4]. In contrast, non-parametric approaches, including the Kaplan-Meier estimator [5], which estimates the survival function, and the Nelson-Aalen estimator, which estimates the cumulative hazard function, derive survival characteristics directly from observed data without assuming explicit distributions. While these methods provide data-driven insights, they lack interpretability regarding the underlying mechanisms driving hazard rate changes and are unable to extrapolate beyond the observed time horizon [6, 7]. Semi-parametric models, such as the Cox proportional hazards model [8], offer a middle ground by allowing covariate effects to be estimated flexibly while leaving the baseline hazard function unspecified. Thus, semi-parametric models are advantageous when the baseline hazard function is unknown but impose other restrictions such as proportional hazards, which may not hold in settings where risk evolves over time. These classical methods thus face limitations in their inability to explicitly model the underlying dynamic mechanisms governing the evolution of the hazard function.

Many real-world survival processes, however, evolve as dynamical systems, where changes in risk depend not only on the current hazard level but also on its rate of change and the surrounding environment. Examples include biological growth and decay processes, disease progression and remission cycles, reliability degradation in engineered systems, and market recovery or failure in economics. Such processes are more naturally described through differential equations than static statistical relationships, motivating the development of dynamical survival analysis. In recent years, ODEs have gained prominence in survival analysis for modeling time-dependent processes. For instance, recent work by Christen and Rubio [9] has introduced systems of ODEs for hazard modeling, shifting the focus from static to dynamic survival analysis. Although first-order ODE systems bridge statistical and mechanistic perspectives, the instantaneous rate of change of the hazard depends only on its current value and time, limiting their ability to represent complex temporal behaviors such as oscillations, delayed feedback, or nonlinear damping [10]. This is particularly relevant in remission–relapse disease courses, fatigue-driven reliability, and recovery from market or environmental shocks, where risk does not merely rise or fall monotonically.

To address these limitations, we propose a novel approach that leverages higher-order ODEs in dynamical survival analysis to model the hazard function. By allowing hazard dynamics to depend on both the current hazard level and its rate of change, the proposed framework captures feedback, inertia, and adaptive responses that are inaccessible to first-order models. Building on this formulation, we develop a collection of nonlinear and oscillatory hazard models. This includes damped oscillatory, sinusoidal, population-dynamics-based, and interaction-moderated exponential hazards, each linking an interpretable dynamical mechanism to an induced survival distribution. In addition, we introduce a general numerical algorithm applicable to all proposed models, enabling solution of higher-order hazard systems, computation of cumulative hazards, and simulation of event times. In addition, we develop likelihood-based inference and moment-generating-function analysis to characterize tail behavior and support estimation under censoring. Finally, we demonstrate the applicability of the framework through simulation studies and a real-data application, showing how higher-order hazard dynamics capture temporal risk patterns that standard monotone models cannot.

In the remainder of this paper, we first formalize the ODE-based modeling framework and review the first-order formulation of hazard dynamics. Building on this foundation, we extend the concept to hazard functions governed by higher-order ODEs, capturing more complex survival

dynamics in Section 2. The probability distribution induced by ODEs is discussed in Section 3. In addition, Section 4 focuses on nonlinear and oscillatory hazard models, demonstrating how higher-order ODEs can represent intricate survival behaviors such as periodic risk patterns and non-monotonic hazard rates. Numerical studies of higher-order ODE-based hazard models and statistical inference are discussed in Sections 5 and 6, respectively. Finally, Section 7 presents a simulation study for higher-order hazard models with application involving real-world survival data illustrated in Section 8.

2 ODE-based Hazard Modeling

This section outlines the proposed ODE-based framework for modeling hazard dynamics. We begin by revisiting the first-order ODE formulation, then extend it to higher-order systems that capture more complex temporal behaviors in survival processes. The approach treats the hazard function and its cumulative form as components of a coupled dynamical system, providing a structured foundation for simulation and inference in later sections.

2.1 First-Order ODE Framework for Hazard Dynamics

We consider a cohort of n subjects with latent event times $\{o_i\}_{i=1}^n$ and right-censoring times $\{c_i\}_{i=1}^n$. In practice, only the earlier of these two times is observed, defined as $t_i = \min(o_i, c_i)$, along with a censoring indicator δ_i , given by:

$$\delta_i = \begin{cases} 1, & o_i \leq c_i, \\ 0, & \text{otherwise.} \end{cases} \quad (1)$$

Each $\{o_i\}$ is assumed to follow a continuous distribution characterized by the following inter-related quantities: a probability density function $f(t)$, a cumulative distribution function $F(t) = \int_0^t f(m) dm$, and a survival function $S(t) = 1 - F(t)$. The hazard function, which describes the instantaneous rate of event occurrence conditional on survival up to time t , is defined as:

$$h(t) = -\frac{S'(t)}{S(t)}, \quad (2)$$

and the cumulative hazard function representing the total accumulated risk up to time t is given by:

$$H(t) = \int_0^t h(m) dm = -\log S(t). \quad (3)$$

To model the temporal evolution of the hazard function explicitly within a dynamical framework, we define a system of first-order ODEs. The instantaneous hazard $h(t)$ is embedded as one component of a vector of dynamically evolving state variables,

$$\mathbf{Y}(t) = (h(t), q_1(t), \dots, q_m(t))^\top, \quad t > 0, \quad (4)$$

where $q_j : \mathbb{R}^+ \rightarrow \mathbb{R}$ ($j = 1, \dots, m$) denotes an auxiliary differentiable function capturing additional latent temporal dynamics in the hazard process. The resulting coupled first-order ODE system governing $\mathbf{Y}(t)$ and the cumulative hazard $H(t)$ is then given by:

$$\begin{aligned}\mathbf{Y}'(t) &= \psi_\theta(\mathbf{Y}(t), t), & \mathbf{Y}(0) &= \mathbf{Y}_0, & H(0) &= 0. \\ H'(t) &= Y_1(t),\end{aligned}\tag{5}$$

where $\psi_\theta : \mathbb{R}^{m+1} \times \mathbb{R}^+ \rightarrow \mathbb{R}^{m+1}$ is a parameterized vector field capturing the dynamic interactions among hazard function components and auxiliary latent processes. The first component, $Y_1(t)$, explicitly represents the instantaneous hazard $h(t)$, ensuring that the cumulative hazard $H(t)$ is consistently and accurately derived from the system. This formulation naturally captures temporal dependencies, nonlinear behavior, and covariate effects in survival dynamics (see, e.g., [11]).

Positivity, Stability, and Structural Constraints Ensuring the nonnegativity of $h(t)$ is essential, since the hazard function is nonnegative by definition. The ODE framework provides several mechanisms for enforcing this property. (a) The vector field ψ_θ can be constructed so that the hazard dynamics preserve nonnegativity, for example by restricting the domain of the system or imposing suitable structural constraints. (b) Alternatively, a transformation such as $\tilde{h}(t) = \log h(t)$ may be used, which guarantees positivity of $h(t)$ while allowing unconstrained evolution of $\tilde{h}(t)$. (c) Finally, initializing the system with $h(0) = h_0 \geq 0$ and enforcing appropriate stability conditions on ψ_θ ensures that nonnegativity is preserved over time.

The inclusion of auxiliary latent states $q_j(t)$ enables the model to capture time-varying covariate effects and latent dependencies in the hazard process, extending the framework to complex survival dynamics. Simultaneous modeling of $h(t)$ and its cumulative counterpart $H(t)$ further ensures internal consistency and facilitates efficient numerical inference. Together, these properties make the ODE framework well suited for modeling complex temporal hazard dynamics, while maintaining key probabilistic constraints [11, 9].

2.2 Higher-Order ODE Frameworks for Hazard Dynamics

We now extend the ODE-based formulation of hazard dynamics from first to higher order, focusing on the second-order case. A graphical abstract is given in Figure 1. Second-order systems introduce an additional degree of freedom that allows the hazard's rate of change itself to evolve dynamically. This added flexibility enables the modeling of acceleration, damping, and feedback effects in the evolution of risk over time.

The hazard function $h(t)$ is modeled as part of a second-order system, with dynamics described by:

$$h''(t) = \phi_\theta(h(t), h'(t), t), \quad t \geq 0, \tag{6}$$

where $\phi_\theta : \mathbb{R}^3 \rightarrow \mathbb{R}$ is a continuously differentiable function parameterized by $\theta \in \Theta \subseteq \mathbb{R}^p$. The function ϕ_θ specifies how the acceleration of the hazard depends on its current value, its instantaneous rate of change, and time. To handle second-order dynamics, the system is conveniently reformulated as a first-order system by introducing an auxiliary variable $v(t) = h'(t)$:

$$\begin{cases} h'(t) = v(t), \\ v'(t) = \phi_\theta(h(t), v(t), t). \end{cases} \tag{7}$$

Define the state vector

$$\mathbf{Y}(t) = \begin{pmatrix} h(t) \\ v(t) \end{pmatrix}, \quad \mathbf{Y}'(t) = \Psi_\theta(\mathbf{Y}(t), t) = \begin{pmatrix} v(t) \\ \phi_\theta(h(t), v(t), t) \end{pmatrix}.$$

which yields a compact state-space representation that retains the flexibility of first-order ODE systems while embedding the richer dynamics of the second order formulation. Second-order systems can naturally capture oscillatory, damped, or feedback-driven behaviors (see, e.g., [12]), which may be relevant in survival scenarios involving cyclical risks, delayed responses, or adaptive mechanisms. These dynamics enable more realistic representations of complex hazard evolution over time.

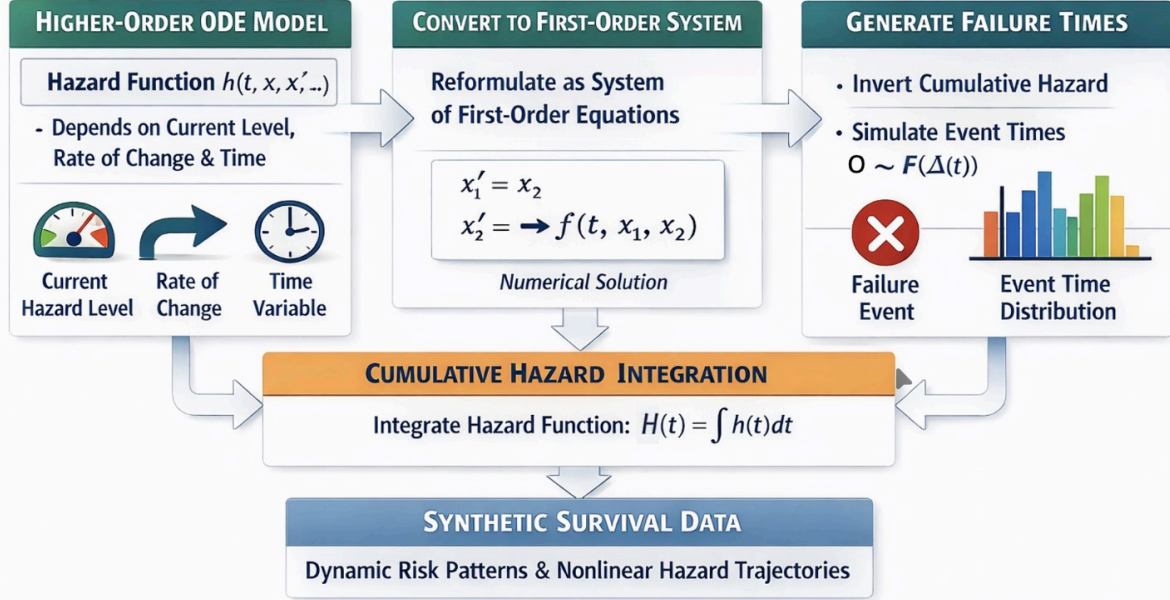


Figure 1: Flowchart illustrating the simulation framework for survival models driven by higher-order dynamical ODEs. The hazard function is modeled using a higher-order ODE, reformulated as a system of first-order equations, numerically solved to obtain the cumulative hazard, and inverted to generate synthetic failure times.

Theorem 1. (Existence, Uniqueness, and Stability of Hazard Dynamics)

Let the hazard function $h(t)$ be governed by a second-order ODE of the form:

$$h''(t) = \phi(h(t), h'(t), t),$$

where $\phi : \mathbb{R}^3 \rightarrow \mathbb{R}$ is a continuous function, and the initial conditions are specified as $h(0) = h_0$ and $h'(0) = v_0$. Assume the following:

1. $\phi(h, h', t)$ is Lipschitz continuous in h and h' , i.e., there exists a constant $L > 0$ such that:

$$|\phi(h_1, v_1, t) - \phi(h_2, v_2, t)| \leq L(|h_1 - h_2| + |v_1 - v_2|), \quad \forall h_1, h_2, v_1, v_2 \in \mathbb{R}, t \geq 0.$$

2. $\phi(h, h', t)$ is bounded for all $t \geq 0$, $h \in \mathbb{R}$, and $h' \in \mathbb{R}$.

Then, there exists a unique solution $h(t)$ defined on an interval $[0, T]$ for the given ODE and initial conditions. For stability, if $\phi(h, h', t)$ is continuously differentiable in h and h' , and if all eigenvalues of the Jacobian matrix of the system:

$$J = \begin{bmatrix} 0 & 1 \\ \frac{\partial \phi}{\partial h} & \frac{\partial \phi}{\partial h'} \end{bmatrix}$$

have negative real parts, then the equilibrium $(h^*, 0)$ is locally asymptotically stable, and $h(t) \rightarrow h^*$ as $t \rightarrow \infty$ for all solutions starting sufficiently close to $(h^*, 0)$.

3 Probability Distribution Induced by First and Second-Order ODEs

In this section, we demonstrate how conventional survival distributions can be interpreted as particular solutions to first- or higher-order ODE systems. Hazard functions $h(t)$ can be naturally expressed as solutions to ODEs. In fact, any continuously differentiable hazard function trivially satisfies the first-order ODE:

$$h'(t) = \psi(h, t),$$

Therefore, a wide class of survival models, both parametric and nonparametric, can be viewed as solutions to dynamical systems characterized by suitable choices of ψ or its higher-order analogues [11, 13, 14]. This dynamical perspective provides a unifying link between conventional probability distributions and the proposed ODE-based framework. Below, we explore representations for both first-order and second-order ODEs, incorporating examples and highlighting their properties.

First-Order ODE Representations We now illustrate how standard survival distributions arise as specific solutions of first-order ODEs. For example, consider the Bernoulli-type differential equation:

$$h'(t) = a(t)h(t) - h(t)^2, \quad (8)$$

where $a(t) = f'(t)/f(t) = (d/dt) \log f(t)$, and $f(t)$ is the probability density function (pdf) of the corresponding survival model. This ODE can also be interpreted as a Riccati-type equation [15]. The coefficient $a(t)$, referred to as the *autonomy coefficient*, determines whether the ODE is autonomous or nonautonomous: (a) If $a(t)$ depends only on $h(t)$, the ODE is autonomous, (b) If $a(t)$ explicitly depends on t , the ODE is non-autonomous.

First-order ODEs with constant or monotonic $a(t)$ often yield hazard functions corresponding to classical monotonic survival distributions. For instance, the Weibull hazard

$$h(t) = \beta \kappa t^{\kappa-1}$$

satisfies

$$a(t) = (\kappa - 1) \left(\frac{\beta \kappa}{h(t)} \right)^{1/(\kappa-1)} - h(t),$$

which corresponds to an autonomous ODE for $\kappa \neq 1$. In contrast, the log-normal distribution, which yields:

$$a(t) = \frac{\mu - \sigma^2 - \log(t)}{\sigma^2 t},$$

making Eq. (8) non-autonomous. Thus, monotonic hazard functions correspond to autonomous scalar ODEs, while non-monotonic hazard behavior necessitates non-autonomous dynamics.

Second-Order ODE Representations and Induced Probability Laws Second-order ODEs provide a richer modeling framework by introducing higher-order dynamics such as acceleration and oscillations. These features are particularly useful for modeling hazard functions with non-monotonic behavior, including periodic or fluctuating risks. A second-order hazard model is given by

$$h''(t) = \phi(h(t), h'(t), t),$$

where ϕ specifies the dependence of the hazard acceleration on its current level, rate of change, and time. Rewriting this system in state-space form,

$$z(t) = h'(t), \quad z'(t) = \phi(h(t), z(t), t),$$

where $z(t)$ denotes the instantaneous rate of change of the hazard.

For each proposed hazard model, the corresponding probability density function is

$$f(t) = h(t) \exp\{-H(t)\}. \quad (9)$$

Random realizations can be generated via inverse transform sampling, with $u \sim \text{Uniform}(0, 1)$ and event times t obtained by solving $H(t) = -\log(1 - u)$.

In the next section, we specify concrete examples of higher-order hazard systems, each illustrating a distinct nonlinear or oscillatory dynamic together with its induced survival and density functions, thereby linking the ODE formulation to empirically relevant survival behavior.

4 Nonlinear and Oscillatory Hazard Models via Higher-Order ODEs

In this section, we consider four representative second-order ODE based hazard models. Although higher-order formulations can be used to describe a wide range of hazard dynamics, we restrict attention to models that arise naturally in time-to-event applications. The models examined are: (1) a damped oscillatory hazard model, (2) a population dynamics-based hazard model, (3) a sinusoidal hazard model, and (4) an exponential hazard model with interaction effects. These models capture common dynamic features such as damping, oscillatory behavior, growth and saturation, and nonlinear interactions, and together provide a flexible class of hazard trajectories.

4.1 Damped Oscillatory Hazard Model

The Damped Oscillatory Hazard Model describes hazard behavior that fluctuates over time with gradually decreasing intensity (see e.g. in [16, 17]). This class of models is particularly useful in settings where the risk does not evolve monotonically but exhibits oscillatory behavior before stabilizing, for example due to adaptation, periodic external factors, or learning before eventually stabilizing (see e.g. [18]). By capturing both cyclical nature and damping effects, this model provides a more realistic and flexible framework to understand time-varying risks in complex systems.

The damped oscillatory hazard model is governed by

$$\phi(h(t), h'(t), t) = -\alpha h'(t) - \beta h(t) + \gamma. \quad (10)$$

Rewriting this in the form of a second-order ODE yields

$$h''(t) + \alpha h'(t) + \beta h(t) = \gamma. \quad (11)$$

The form of the solution is determined by the discriminant $\Delta = \alpha^2 - 4\beta$ of the characteristic equation $r^2 + \alpha r + \beta = 0$, leading to three distinct cases: underdamped ($\Delta < 0$), critically damped ($\Delta = 0$), and overdamped ($\Delta > 0$).

Case 1: Underdamped ($\Delta < 0$)

For the underdamped case $\Delta = \alpha^2 - 4\beta < 0$, the characteristic equation has complex conjugate roots,

$$r_{1,2} = -\frac{\alpha}{2} \pm i\omega, \quad \omega = \frac{1}{2}\sqrt{4\beta - \alpha^2}.$$

To solve Eq. 11, the general solution for $h(t)$ in the case ($\Delta < 0$) can be written as

$$h(t) = e^{-\frac{\alpha t}{2}} (A \cos(\omega t) + B \sin(\omega t)) + h^*, \quad h^* = \frac{\gamma}{\beta},$$

where h^* is the equilibrium hazard. Applying the initial conditions $h_0 = h(0)$ and $v_0 = h'(0)$, the constants A and B are obtained as

$$A = h_0 - \frac{\gamma}{\beta}, \quad B = \frac{1}{\omega} \left(v_0 + \frac{\alpha}{2} \left(h_0 - \frac{\gamma}{\beta} \right) \right).$$

The value h_0 represents the initial hazard level, and v_0 denotes the initial rate of change of the hazard. The coefficient α is the damping parameter, which determines the rate at which the oscillations decay over time. The term ω is the angular frequency that determines the speed of oscillation, and γ/β is the long-run equilibrium hazard level.

Case 2: Critically Damped ($\Delta = 0$)

In the critically damped case $\Delta = 0$, the characteristic equation has a repeated root $r = -\alpha/2$. The solution of Eq. 11 therefore takes the form:

$$h(t) = (A + Bt)e^{-\alpha t/2} + \frac{\gamma}{\beta}.$$

The constants A and B follow from the intial conditions $h_0 = h(0)$ and $v_0 = h'(0)$:

$$A = h_0 - \frac{\gamma}{\beta}, \quad B = v_0 + \frac{\alpha}{2} \left(h_0 - \frac{\gamma}{\beta} \right)$$

In this setting, α serves as the critical damping coefficient and determines the rate at which the hazard approaches equilibrium without oscillation. Under the critical damping condition, the restoring coefficient β satisfies $\beta = \alpha^2/4$.

Case 3: Overdamped ($\Delta > 0$)

For the overdamped case $\Delta > 0$, the characteristic equation has two real and distinct roots,

$$r_{1,2} = -\frac{\alpha}{2} \pm \sqrt{\frac{\alpha^2}{4} - \beta}.$$

The corresponding solution to Eq. 11 is

$$h(t) = Ae^{r_1 t} + Be^{r_2 t} + \frac{\gamma}{\beta},$$

where the constants A and B are determined by the initial conditions $h_0 = h(0)$ and $v_0 = h'(0)$. In this case, the hazard returns to its equilibrium level γ/β without oscillation, but at a slower

rate than under critical damping. The two exponential terms reflect two different decay speeds associated with the distinct roots r_1 and r_2 .

In Figure 2, we illustrate the typical behavior of the three damping cases. The underdamped case shows oscillations in the hazard before settling, the critically damped case returns to equilibrium smoothly without oscillation, and the overdamped case approaches equilibrium more slowly. These differences produce small early-time variations in the survival curves, while the long-run behavior is similar across all three cases.

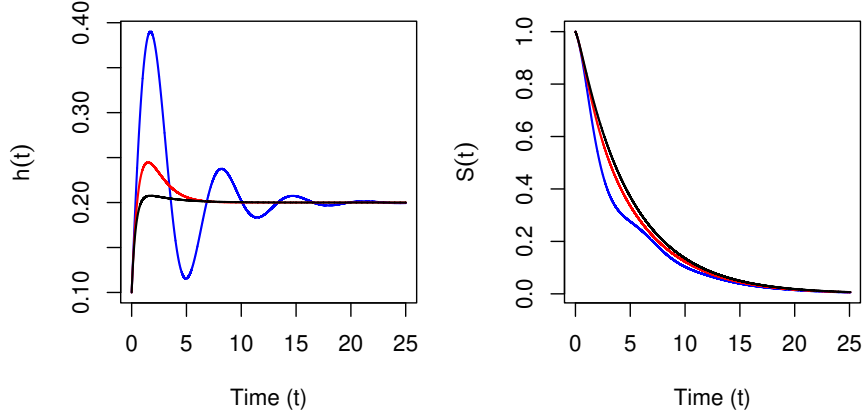


Figure 2: Hazard functions $h(t)$ and survival functions $S(t)$ for the damped oscillatory model under the underdamped ($\alpha = 0.5$, $\beta = 1$, $\gamma = 0.2$, $h_0 = 0.1$, $v_0 = 0.3$; blue), critically damped ($\alpha = 2$, $\beta = 1$, $\gamma = 0.2$, $h_0 = 0.1$, $v_0 = 0.3$; red), and overdamped ($\alpha = 3$, $\beta = 1$, $\gamma = 0.2$, $h_0 = 0.1$, $v_0 = 0.3$; black) cases.

For each case described earlier, the cumulative hazard function $H(t)$ is obtained by integrating the corresponding hazard function $h(t)$. In the underdamped case ($\Delta < 0$), this yields:

$$H(t) = \int_0^t \left[e^{-\alpha u/2} (A \cos(\omega u) + B \sin(\omega u)) + \frac{\gamma}{\beta} \right] du.$$

This expression simplifies to the following closed form:

$$\begin{aligned} H(t) = & \frac{\gamma}{\beta} t + \frac{A}{\beta} \left[\frac{\alpha}{2} + e^{-\alpha t/2} \left(-\frac{\alpha}{2} \cos(\omega t) + \omega \sin(\omega t) \right) \right] \\ & + \frac{B}{\beta} \left[\omega + e^{-\alpha t/2} \left(-\frac{\alpha}{2} \sin(\omega t) - \omega \cos(\omega t) \right) \right]. \end{aligned}$$

The density function is then obtained by combining the hazard and cumulative hazard functions as $f(t) = h(t) \exp\{-H(t)\}$. Then, using the inverse transform sampling approach, event times can be simulated for the underdamped case. A similar numerical procedure applies to the remaining cases, with the specific implementation depending on the forms of $h(t)$ and $H(t)$.

Theorem 2. (Long-Term Behavior of the Damped Oscillatory Hazard)

Consider the damped oscillator Eq. 11, with initial conditions $h(0) = h_0 > 0$ and $h'(0) = v_0$. Assume the unique solution satisfies $h(t) > 0$ for all $t \geq 0$. Then:

1. **Existence and Uniqueness:** For any $h_0 > 0$ and $v_0 \in \mathbb{R}$, there exists a unique solution $h(t)$ defined for all $t \geq 0$.

2. **Asymptotic Stability:** For any $\alpha > 0$ and $\beta > 0$, the equilibrium $h^* = \gamma/\beta$ is globally asymptotically stable, and

$$\lim_{t \rightarrow \infty} h(t) = h^* = \frac{\gamma}{\beta}.$$

3. **Damping Regimes:** Let $\Delta = \alpha^2 - 4\beta$.

- If $\Delta < 0$, the solution exhibits oscillations about h^* with exponentially decaying amplitude (underdamped).
- If $\Delta = 0$, the solution converges to h^* at the critical damping rate.
- If $\Delta > 0$, the solution converges monotonically to h^* as a sum of decaying exponentials (overdamped).

Proof. The proof is given in Appendix B. \square

4.2 Population Dynamics-Based Hazard Model

The classical logistic growth law is widely used in ecology to describe how a population grows when resources are limited [19, 20]. In its standard first-order form, the dynamics are

$$h'(t) = r h(t) \left(1 - \frac{h(t)}{K}\right), \quad (12)$$

where $r > 0$ is the intrinsic growth rate and $K > 0$ is the carrying capacity. The analytic solution is the familiar sigmoidal curve

$$h(t) = \frac{K h_0 e^{rt}}{K + h_0(e^{rt} - 1)},$$

showing that in the first-order logistic formulation the trajectory of $h(t)$ is determined entirely by its current value [21]. Because Eq. (12) specifies only the instantaneous slope, it reacts immediately to the current state and cannot capture inertia or acceleration. As a result, it cannot generate overshoot, oscillations, or transient amplification.

To encode inertia and state-dependent acceleration, we propose the nonlinear second-order logistic system

$$h''(t) = \phi(h(t), h'(t), t) = r h(t) \left(1 - \frac{h(t)}{K}\right). \quad (13)$$

Here the logistic feedback acts directly on the acceleration of the hazard. In contrast to the recent harmonic-oscillator hazard of [22], which is a linear second-order ODE with a closed form solution, our model Eq. (13) is *nonlinear* and autonomous. Transient dynamics (overshoot, oscillations, non-monotone adjustment toward K) arise from the logistic mechanism itself rather than from a linear restoring force.

Since Eq. (13) has no simple closed-form solution, we introduce $v(t) = h'(t)$ and rewrite it as a first-order system:

$$\begin{cases} h'(t) = v(t), \\ v'(t) = r h(t) \left(1 - \frac{h(t)}{K}\right), \end{cases} \quad h(0) = h_0, \quad v(0) = v_0. \quad (14)$$

For numerical simulation we include a small damping term $\eta h'(t)$, $\eta > 0$, giving

$$h''(t) + \eta h'(t) = r h(t) \left(1 - \frac{h(t)}{K}\right),$$

which prevents sustained oscillations and stabilizes convergence to K . Equivalently, this can be written as

$$\begin{cases} h'(t) = v(t), \\ v'(t) = r h(t) \left(1 - \frac{h(t)}{K}\right) - \eta v(t), \end{cases} \quad h(0) = h_0, \quad v(0) = v_0. \quad (15)$$

For sufficiently large damping, numerical solutions initiated with $h_0 > 0$ remain positive and converge to K for the range of initial conditions considered. Accordingly, in the simulation study we restrict attention to $h_0 > 0$ and $\eta > 0$ for which the numerical solution satisfies $h(t) \geq 0$ for all t ; all simulations reported meet this requirement.

To better understand the dynamical role of the parameters, we rescale

$$x(t) = \frac{h(t)}{K}, \quad \tau = \sqrt{r} t,$$

which converts the damped second-order logistic equation into

$$\frac{d^2x}{d\tau^2} + \zeta \frac{dx}{d\tau} = x(1 - x), \quad \zeta = \frac{\eta}{\sqrt{r}}.$$

Thus, the transient behavior of the second-order hazard depends on the damping parameter ζ . Large damping ($\zeta \gg 1$) produces monotone convergence, while weak damping ($\zeta \ll 1$) yields overshoot and oscillatory adjustment toward $x = 1$ (i.e., $h(t) = K$). Damping only governs the decay rate of oscillations; the inertia-driven overshoot is retained.

Classical extensions of the logistic law generate non-monotone trajectories by adding *memory*. A delayed logistic model,

$$h'(t) = r h(t) \left(1 - \frac{h(t - \tau)}{K}\right), \quad (16)$$

produces overshoot or oscillation when the delay τ is sufficiently large, because the system reacts to the past state $h(t - \tau)$ [23, 24, 25]. Here, complex behavior is driven by history. Our second-order model Eq. (13) produces similar transient effects (overshoot, oscillation) *without delay*: inertia replaces memory in driving transient instability.

Figure 3 illustrates these differences: the first-order model converges monotonically, the delayed model overshoots due to feedback on a past state, and the second-order model overshoots because acceleration carries the system beyond K before it slows down.

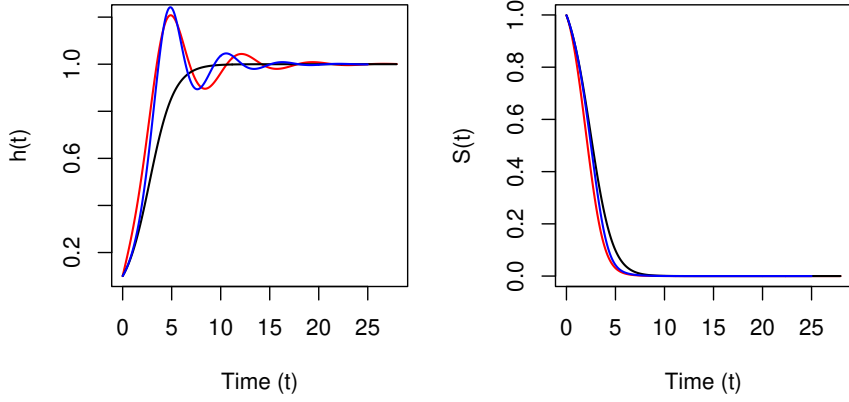


Figure 3: Hazard functions $h(t)$ and survival functions $S(t)$ for logistic hazard dynamics between first-order (black), delayed (blue), and damped second-order logistic (red) hazard models ($r = 0.8$, $K = 1$, $\tau = 1.2$, $\zeta = 0.5$, $h_0 = 0.1$, $v_0 = 0.2$).

4.3 Sinusoidal Hazard Model

Standard hazard models, such as the exponential and Weibull, assume constant or monotonic hazard functions [26]. However, in many real-world situations, the hazard may vary periodically due to factors like seasonal changes or biological rhythms [27, 28, 29]. In such cases, sinusoidal hazard models provide a natural alternative by capturing these recurring risk patterns over time. This model is particularly well suited for contexts involving periodic or cyclical hazard behavior, including seasonal effects on survival (e.g., weather-related risk variations), recurring health events (e.g., annual epidemics), and cyclical influences from market or environmental conditions. Unlike the damped oscillatory hazard model, which exhibits decaying fluctuations over time due to damping, the sinusoidal model preserves constant amplitude and frequency throughout the time domain.

The sinusoidal hazard model is defined by the second-order ODE

$$h''(t) = \phi(h(t), h'(t), t) = -\omega^2 h(t)$$

whose general solution is $h(t) = A \cos(\omega t) + B \sin(\omega t)$.

Since this form oscillates around zero and may take negative values, we introduce a constant shift (c) to ensure $h(t) > 0$ for all t . We therefore consider the modified equation

$$h''(t) = -\omega^2(h(t) - c). \quad (17)$$

with solution

$$h(t) = A \cos(\omega t) + B \sin(\omega t) + c \quad (18)$$

The parameter ω controls the oscillation frequency, and c is the baseline hazard level, capturing the persistent risk level that remains constant regardless of the cyclical fluctuations. The oscillatory component has amplitude $R = \sqrt{A^2 + B^2}$, so the hazard fluctuates around c with amplitude R . Given initial conditions $h(0) = h_0$ and $h'(0) = v_0$, the solution can be written as

$$h(t) = (h_0 - c) \cos(\omega t) + \frac{v_0}{\omega} \sin(\omega t) + c, \quad (19)$$

in which case the amplitude reduces to

$$R = \sqrt{(h_0 - c)^2 + \left(\frac{v_0}{\omega}\right)^2},$$

and the minimum of the hazard over time is therefore $\min_t h(t) = c - R$. For $h_0 > 0$, strict positivity of $h(t)$ for all t is equivalent to

$$c > \frac{h_0}{2} + \frac{v_0^2}{2h_0\omega^2}.$$

The corresponding cumulative hazard function follows from integration of $h(t)$ and it is given by

$$H(t) = ct + \frac{h_0 - c}{\omega} \sin(\omega t) + \frac{v_0}{\omega^2} \{1 - \cos(\omega t)\}.$$

The pdf is

$$f(t) = \left(c + (h_0 - c) \cos(\omega t) + \frac{v_0}{\omega} \sin(\omega t) \right) \exp \left(-ct - \frac{h_0 - c}{\omega} \sin(\omega t) - \frac{v_0}{\omega^2} (1 - \cos(\omega t)) \right).$$

Figure 4 illustrates the typical behavior of the sinusoidal hazard model. In contrast to the oscillatory hazard model, which eventually converges to a steady level, the sinusoidal hazard model continues to fluctuate over time and does not settle to a constant value. This model is therefore appropriate in settings where risk follows a recurring pattern rather than approaching equilibrium. By allowing persistent fluctuations around a baseline level, the sinusoidal hazard captures temporal structure that cannot be represented by hazard models that converge to a steady state.

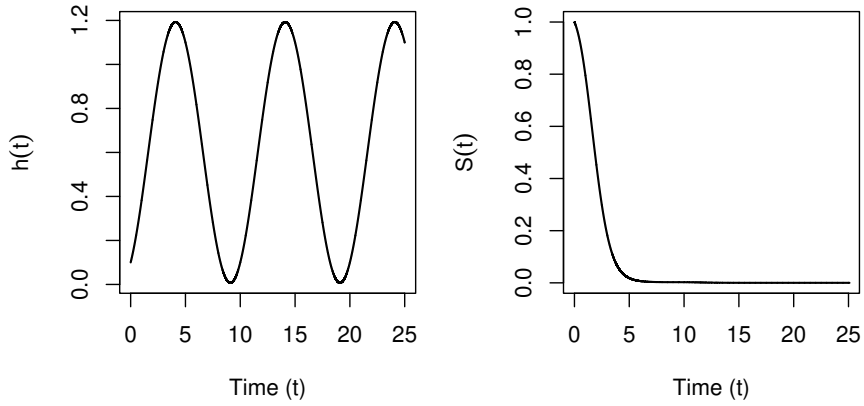


Figure 4: Hazard function $h(t)$ and survival function $S(t)$ for the sinusoidal hazard model ($h_0 = 0.1$, $v_0 = 0.2$, $\omega = 0.2\pi$, $c = 0.6$).

4.4 Exponential Hazard Model with Interaction

The exponential function is central to modeling dynamic processes in physics and biology, including population growth, tumor development, sterilization effects, and drug kinetics. However, exponential growth cannot continue indefinitely due to constraints such as limited nutrients or environmental capacity. To capture such phenomena with greater flexibility, the exponential growth and

decay with interaction model extends the basic exponential framework by incorporating additional parameters. In this section, we will discuss only exponential growth.

We define an exponential hazard model with interaction through the second-order ODE

$$h''(t) = \phi(h(t), h'(t), t) = \alpha h(t) - \beta (h'(t))^2. \quad (20)$$

Here, the interaction term refers to the nonlinear coupling involving $h'(t)$. The inclusion of this term moderates the growth of the hazard relative to the case $\beta = 0$.

For analysis and computation, Eq. 20 may be written as the equivalent first-order system

$$\begin{cases} h'(t) = v(t), \\ v'(t) = \alpha h(t) - \beta v(t)^2 \end{cases} \quad h(0) = h_0, \quad v(0) = v_0. \quad (21)$$

The model is parameterized by $(h_0, v_0, \alpha, \beta)$, where $h_0 = h(0)$ and $v_0 = h'(0)$ specify the initial condition. The parameter α governs the growth component of the hazard, while β introduces a nonlinear interaction through the rate of change $h'(t)$. The associated quadratic term acts as a damping mechanism that becomes more pronounced when $h'(t)$ is large, thereby moderating the growth of $h(t)$.

Special Case: when $\beta = 0$

When $\beta = 0$, the interaction term vanishes and the model reduces to the linear second-order equation

$$h''(t) = \alpha h(t). \quad (22)$$

For $\alpha > 0$, the solution of Eq. (22) is a linear combination of exponentially increasing and decreasing components, and the long-term behavior of $h(t)$ is dominated by the exponentially increasing component. When $\alpha < 0$, the solution is oscillatory. We therefore restrict attention to $\alpha > 0$, which isolates the exponential mechanism and provides a natural reference for comparison with the model in Eq. (20) when $\beta > 0$. The general solution of Eq. (22) in this case can be written as

$$h(t) = Ae^{\sqrt{\alpha}t} + Be^{-\sqrt{\alpha}t},$$

where the constants A and B are determined by the initial conditions $h(0) = h_0$ and $h'(0) = v_0$. Solving for A and B gives

$$A = \frac{1}{2} \left(h_0 + \frac{v_0}{\sqrt{\alpha}} \right), \quad B = \frac{1}{2} \left(h_0 - \frac{v_0}{\sqrt{\alpha}} \right).$$

Thus,

$$h(t) = \frac{1}{2} \left(h_0 + \frac{v_0}{\sqrt{\alpha}} \right) e^{\sqrt{\alpha}t} + \frac{1}{2} \left(h_0 - \frac{v_0}{\sqrt{\alpha}} \right) e^{-\sqrt{\alpha}t}.$$

For $\alpha > 0$, the sign of $h(t)$ is determined by the coefficients in its exponential representation. Since $e^{\pm\sqrt{\alpha}t} > 0$ for all $t \geq 0$, $h(t)$ remains positive for all $t \geq 0$ if and only if

$$h_0 + \frac{v_0}{\sqrt{\alpha}} \geq 0 \quad \text{and} \quad h_0 - \frac{v_0}{\sqrt{\alpha}} \geq 0,$$

or equivalently,

$$h_0 \geq \frac{|v_0|}{\sqrt{\alpha}}.$$

If this condition is violated, one of the coefficients becomes negative and the resulting solution eventually takes negative values, which is incompatible with the definition of the hazard function. Moreover, when $h_0 > 0$, $\alpha > 0$, and $v_0 < 0$ satisfy $h_0 = -v_0/\sqrt{\alpha}$, the coefficient of the growing exponential term vanishes, and the hazard reduces to

$$h(t) = h_0 e^{-\sqrt{\alpha}t}.$$

which is positive and strictly decreasing for all $t \geq 0$ (see Figure 5). As $t \rightarrow \infty$, $h(t)$ converges to zero and $H(t)$ approaches the finite limit $h_0/\sqrt{\alpha}$. Consequently, $S(t)$ converges to a positive constant, indicating an improper survival distribution with a nonzero long-term survival probability.

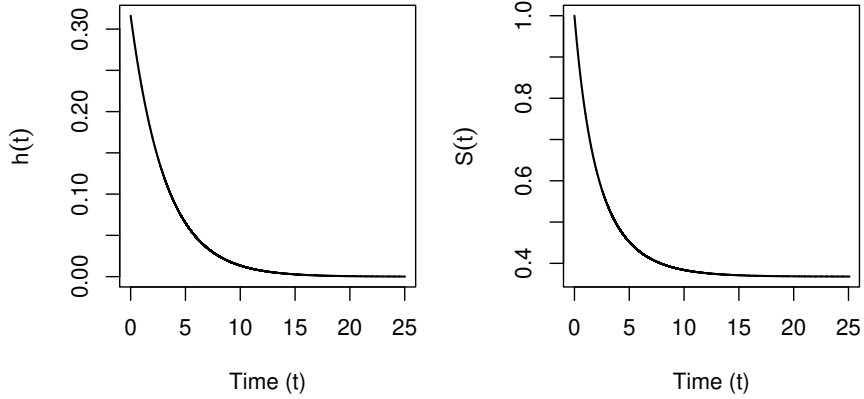


Figure 5: Hazard function $h(t)$ and survival function $S(t)$ for the exponential hazard model ($\alpha = 0.1$, $v_0 = -0.1$).

With $h(t)$ available in closed form, the cumulative hazard function for Eq. (22) is given by

$$H(t) = \frac{1}{2\sqrt{\alpha}} \left(h_0 + \frac{v_0}{\sqrt{\alpha}} \right) \left(e^{\sqrt{\alpha}t} - 1 \right) + \frac{1}{2\sqrt{\alpha}} \left(h_0 - \frac{v_0}{\sqrt{\alpha}} \right) \left(1 - e^{-\sqrt{\alpha}t} \right)$$

Using $h(t)$ and $H(t)$, the pdf of the event time can be derived and used for simulation.

General Case: when $\beta > 0$

For $\beta > 0$, the nonlinear damping term remains and the hazard dynamics are governed by Eq. (20). In this case, no closed-form analytic solution is available, and the solution must be obtained numerically for given initial conditions. Numerical solutions for hazard models without closed-form expressions can be obtained using standard ODE solvers, such as Runge-Kutta methods (see, e.g., [30, 31]), with specified initial conditions and sufficiently small step sizes to ensure numerical stability and accuracy. Figure 6 illustrates the behavior of the exponential hazard model for $\beta = 0$ and $\beta > 0$. Introducing the interaction term moderates the growth of the hazard, resulting in a slower increase in $h(t)$ compared with the case $\beta = 0$. This change in hazard dynamics is also reflected in the survival functions, where the interaction affects both the timing and the rate of survival decay.

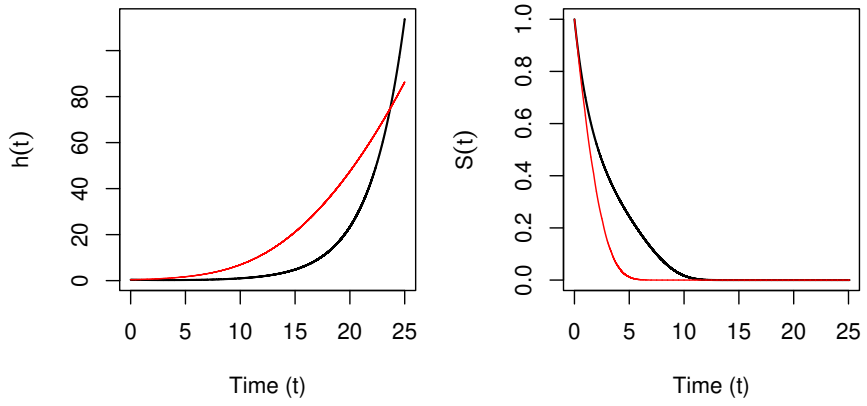


Figure 6: Hazard function $h(t)$ and survival function $S(t)$ for the exponential hazard model ($\alpha = 0.1$, $h_0 = 0.4$, $v_0 = 0.1$; black) and the exponential hazard model with interaction ($\alpha = 0.1$, $\beta = 0.1$, $h_0 = 0.4$, $v_0 = 0.1$; red).

5 Numerical Algorithm for Higher Order ODE-Based Hazard Models

In this, we describe a general numerical algorithm applicable to all proposed ODE-based hazard models. This algorithm provides a general framework for solving the corresponding systems of second-order ODEs, and generating survival time realizations. It is flexible enough to accommodate the specific structure of each model and can be implemented using standard solvers such as Runge-Kutta method.

Algorithm 1 Numerical Simulation of Second-Order ODE: $h''(t) = \phi_\theta(h(t), h'(t), t)$

Require: Model parameters θ , initial values $h(t_0)$ and $v(t_0) = h'(t_0)$, time interval $[t_0, T]$, step size Δt

Ensure: Discrete trajectories of $h(t)$, $v(t)$, cumulative hazard $H(t)$, and simulated failure time t^*

1: Define uniform time grid: $t_i = t_0 + i \cdot \Delta t$ for $i = 0, 1, \dots, N$ such that $t_N = T$

2: Initialize:

$$h_0 \leftarrow h(t_0), \quad v_0 \leftarrow v(t_0), \quad H_0 \leftarrow 0$$

3: **for** $i = 1$ to N **do**

4: Solve the system of first-order ODEs:

$$\begin{cases} \frac{dh}{dt} = v(t) \\ \frac{dv}{dt} = \phi_\theta(h(t), v(t), t) \end{cases}$$

from $t = t_{i-1}$ to $t = t_i$ using 4th-order Runge-Kutta:

1. Compute RK4 steps k_1, k_2, k_3, k_4 for both h and v

2. Update:

$$h_i \leftarrow h_{i-1} + \frac{\Delta t}{6}(k_{1h} + 2k_{2h} + 2k_{3h} + k_{4h})$$
$$v_i \leftarrow v_{i-1} + \frac{\Delta t}{6}(k_{1v} + 2k_{2v} + 2k_{3v} + k_{4v})$$

5: Compute cumulative hazard at t_i using trapezoidal rule:

$$H_i \leftarrow H_{i-1} + \frac{1}{2} (h_{i-1} + h_i) \Delta t$$

6: **end for**

7: **Simulate failure time:**

8: Draw $u \sim \text{Uniform}(0, 1)$

9: Solve for t^* such that:

$$H(t^*) = -\log(1 - u)$$

using root-finding (e.g., bisection or `uniroot()` in R), based on interpolating the discrete cumulative hazard trajectory $\{(t_i, H_i)\}$

10: **return** Arrays $\{h_i\}_{i=0}^N$, $\{v_i\}_{i=0}^N$, $\{H_i\}_{i=0}^N$, and simulated failure time t^*

6 Inference

Moments and moment generating functions (MGFs) are commonly used in survival analysis to describe the distribution of failure times and to support inference on quantities such as the mean survival time and variability [32, 33]. In degradation-threshold models, MGFs are also used to study first-passage time distributions, which determine the associated hazard and survival functions. In addition, parameter estimation for the proposed hazard models is carried out using maximum likelihood estimation (MLE), which provides a principled framework for inference based on observed event times and censoring. In this section, we focus on moment generating functions and likelihood-based inference for proposed hazard models defined through higher-order ordinary

differential equations.

6.1 Moment Generating Function

Let T denote a non-negative random variable with density $f(t)$ defined in Eq. 9. The MGF of T is given by

$$M_T(s) = \mathbb{E}[e^{sT}] = \int_0^\infty e^{st} f(t) dt$$

for all s in the set for which the integral exists.

For the hazard models considered in this work, the existence and domain of the MGF depend on the asymptotic behavior of $H(t)$. Since $h(t) \geq 0$, $H(t)$ is monotone increasing and its asymptotic growth rate determines the tail behavior and the existence of the MGF. Closed-form expressions for $M_T(s)$ are generally unavailable for the proposed hazard models, and numerical integration is therefore required. Nevertheless, the existence of the MGF can be characterized for each model based on the asymptotic behavior of $H(t)$, as discussed below.

For the damped oscillatory hazard model, Theorem 2 shows that $h(t) \rightarrow \gamma/\beta$ as $t \rightarrow \infty$ under $\alpha > 0$ and $\beta > 0$. Consequently, the cumulative hazard satisfies

$$H(t) \sim (\gamma/\beta)t \quad \text{as } t \rightarrow \infty,$$

implying exponential tail decay of the corresponding survival distribution. It follows that $M_T(s)$ exists for all $s < \gamma/\beta$ and diverges for $s \geq \gamma/\beta$.

For $\eta > 0$, solutions of the population dynamics-based hazard equation converge to the equilibrium K as $t \rightarrow \infty$. Consequently, $H(t) \approx Kt$ as $t \rightarrow \infty$. This implies that $S(t) \approx e^{-Kt}$ for large t , and that the moment generating function $M_T(s)$ exists for all $s < K$ and diverges for $s > K$.

For the sinusoidal hazard model with parameters chosen such that $h(t) > 0$ for all $t \geq 0$, the cumulative hazard can be written as

$$H(t) = ct + O(1) \quad \text{as } t \rightarrow \infty.$$

The oscillatory terms in $h(t)$ are bounded and therefore contribute only bounded fluctuations to $H(t)$, without affecting its linear growth rate. Consequently, the $S(t)$ decays exponentially at rate c . This tail behavior determines the existence of MGF. When $s < c$, the exponential decay of the survival distribution dominates the growth of the factor e^{sT} , and the integral defining $M_T(s)$ converges. When $s \geq c$, the growth of e^{sT} overwhelms the tail decay, causing the integral to diverge. As a result, $M_T(s)$ exists for all $s < c$ and diverges for $s \geq c$.

For the exponential hazard model with an interaction term, when $\beta = 0, \alpha > 0$, $H(t)$ admits a closed-form expression and grows exponentially in t , provided that $h_0 + v_0/\sqrt{\alpha} > 0$. In particular,

$$H(t) \sim C e^{\sqrt{\alpha}t} \quad \text{as } t \rightarrow \infty,$$

for some constant $C > 0$. Consequently, the rapid decay of the survival function implies that $M_T(s)$ exists and is finite for all $s \in \mathbb{R}$. In the boundary case $h_0 + v_0/\sqrt{\alpha} = 0$, the leading exponential term in $H(t)$ vanishes and $H(t)$ remains bounded. Consequently, $S(\infty) > 0$, implying a positive probability that the event does not occur. In this case, $T = \infty$ with positive probability, and $M_T(s)$ is infinite for all $s > 0$.

6.2 Maximum Likelihood Estimation

Due to the parametric structure of the proposed hazard models, the log-likelihood function can be expressed in terms of the hazard and cumulative hazard functions as

$$l(\boldsymbol{\theta}, \mathbf{Y}_0) = \sum_{i=1}^n \delta_i \log h(t_i | \boldsymbol{\theta}, \mathbf{Y}_0) - \sum_{i=1}^n H(t_i | \boldsymbol{\theta}, \mathbf{Y}_0),$$

where $\boldsymbol{\theta}$ denotes the vector of model parameters, chosen such that $h(t) > 0$ for all $t \geq 0$, and \mathbf{Y}_0 denotes the vector of initial conditions, which are treated as unknown parameters. Although initial conditions may be partially informed by available data, specifying fixed values (e.g., h_0) can be challenging. We therefore treat \mathbf{Y}_0 as model parameters and estimate them jointly with $\boldsymbol{\theta}$.

Given the hazard function $h(t)$ for the proposed models, the log-likelihood can be evaluated for any candidate parameter value. MLEs for both $\boldsymbol{\theta}$ and \mathbf{Y}_0 are then obtained using general-purpose numerical optimization routines, such as `optim` or `nlminb` in R.

In addition to MLE, a Bayesian approach offers a natural extension for inference in this setting. Survival data often involve censoring, limited follow-up, or small sample sizes, which can make likelihood-based estimates unstable or less informative. A Bayesian framework helps address these challenges by incorporating prior knowledge and producing full posterior distributions for the unknown parameters. However, a key challenge in Bayesian implementation lies in selecting appropriate prior distributions for model parameters, which can vary across different hazard structures. Prior selection remains a challenge, but parameter interpretability often supports the use of informative or weakly informative priors. To implement this framework in practice, efficient sampling from the posterior is essential. Since the likelihood is tractable at each parameter value, either analytically or numerically, the proposed models are compatible with general purpose sampling algorithms. Posterior inference can be performed using standard MCMC methods, such as Metropolis-within-Gibbs (`BUGS`, `spBayes`), Hamiltonian Monte Carlo (`Stan`), or adaptive samplers like `twalk` and `MCMCPack`. Details of the Monte Carlo simulation procedure are provided in Appendix C.

7 Simulation Study

In this section, we present simulation results to evaluate the performance of the proposed hazard models described in section 4. For this purpose, data were simulated from the proposed models under fixed parameter settings.

1. Damped oscillatory hazard model,
 - (a) Underdamped: $\alpha = 0.5$, $\beta = 1$, $\gamma = 0.2$, $h_0 = 0.1$, $v_0 = 0.3$
 - (b) Critically damped: $\alpha = 3$, $\gamma = 0.2$, $h_0 = 0.1$, $v_0 = 0.3$
 - (c) Overdamped: $\alpha = 3$, $\beta = 1$, $\gamma = 0.2$, $h_0 = 0.1$, $v_0 = 0.3$
2. Population dynamics-based hazard model: $r = 0.8$, $\zeta = 0.5$, $K = 1$, $h_0 = 0.1$, $v_0 = 0.2$,
3. Sinusoidal hazard model: $\omega = 0.2\pi$, $c = 0.6$, $h_0 = 0.1$, $v_0 = 0.2$
4. Exponential hazard model with interaction effects : $\alpha = 0.1$, $h_0 = 0.4$, $v_0 = 0.1$

To assess performance, 20,000 Monte Carlo replications were generated for each model using sample sizes of 500, 1000, 2000, and 5000. Independent right censoring was imposed by generating censoring times from a uniform distribution, with observed times defined as $t = \min(T, C)$ and event indicators $\delta = \mathbb{I}(T \leq C)$, resulting in censoring rates of approximately 20% to 30%.

For each simulated dataset, model parameters were estimated via Bayesian framework using the t-walk sampler implemented in R. Weakly informative prior distributions were adopted for all model parameters; in particular, positive-valued parameters were assigned $\text{Gamma}(2, 2)$ priors to provide mild regularization while retaining flexibility. To obtain posterior samples, 110,000 Markov chain Monte Carlo (MCMC) iterations were run. The first 10,000 iterations were discarded as burn-in, and a thinning interval of 5 was applied by retaining every fifth draw to reduce autocorrelation, yielding 20,000 samples for posterior inference. Model performance was summarized across Monte Carlo replications using posterior means and root mean squared errors (RMSE) to examine estimation accuracy under different sample sizes.

Table 1 reports the posterior means and RMSEs for each parameter of the underdamped hazard model. As expected, RMSEs decrease with increasing sample size, indicating improved estimation accuracy and consistency. Figure 7 displays the posterior distributions of the model parameters for the underdamped hazard model when the sample size is $n = 2000$. Compared to the corresponding priors (shown in red), the posterior distributions are more concentrated, reflecting increased information from the data at this sample size. Similar summaries for the remaining models proposed in section 4 are provided in the Appendix D.

Table 1: Posterior Results for the underdamped hazard model. True parameter values are shown in parentheses.

		$\alpha (0.5)$	$\beta (1)$	$\gamma (0.2)$	$h_0 (0.1)$	$v_0 (0.3)$
$n = 200$	Mean	0.5821	1.0219	0.2003	0.0891	0.4339
	RMSE	0.2783	0.1860	0.0553	0.0473	0.1870
$n = 500$	Mean	0.7425	1.2398	0.2700	0.0728	0.3646
	RMSE	0.3813	0.3710	0.1080	0.0399	0.1251
$n = 1000$	Mean	0.4197	1.0985	0.2286	0.0975	0.2597
	RMSE	0.1791	0.1511	0.0452	0.0225	0.0714
$n = 2000$	Mean	0.3778	1.0697	0.2315	0.1010	0.2780
	RMSE	0.1540	0.0930	0.0372	0.0166	0.0456
$n = 5000$	Mean	0.5335	0.9635	0.1885	0.0914	0.3156
	RMSE	0.0778	0.0635	0.0186	0.0137	0.0326

8 Real Data Application

To illustrate the use of the proposed methods in real-life applications, we apply the sinusoidal hazard model (Eq. (19)) to the well-known `lung` survival dataset from the `survival` package in R. The dataset consists of 228 subjects with advanced lung cancer from the North Central Cancer Treatment Group. In this cohort, initiation and cycles of systemic therapy, recovery-toxicity phases, and changes in clinical monitoring can induce temporal fluctuations in the instantaneous risk of death, rather than a strictly monotone or single-peak pattern. The sinusoidal baseline provides a parsimonious representation of such alternating risk levels, modeling deviations around a long-run

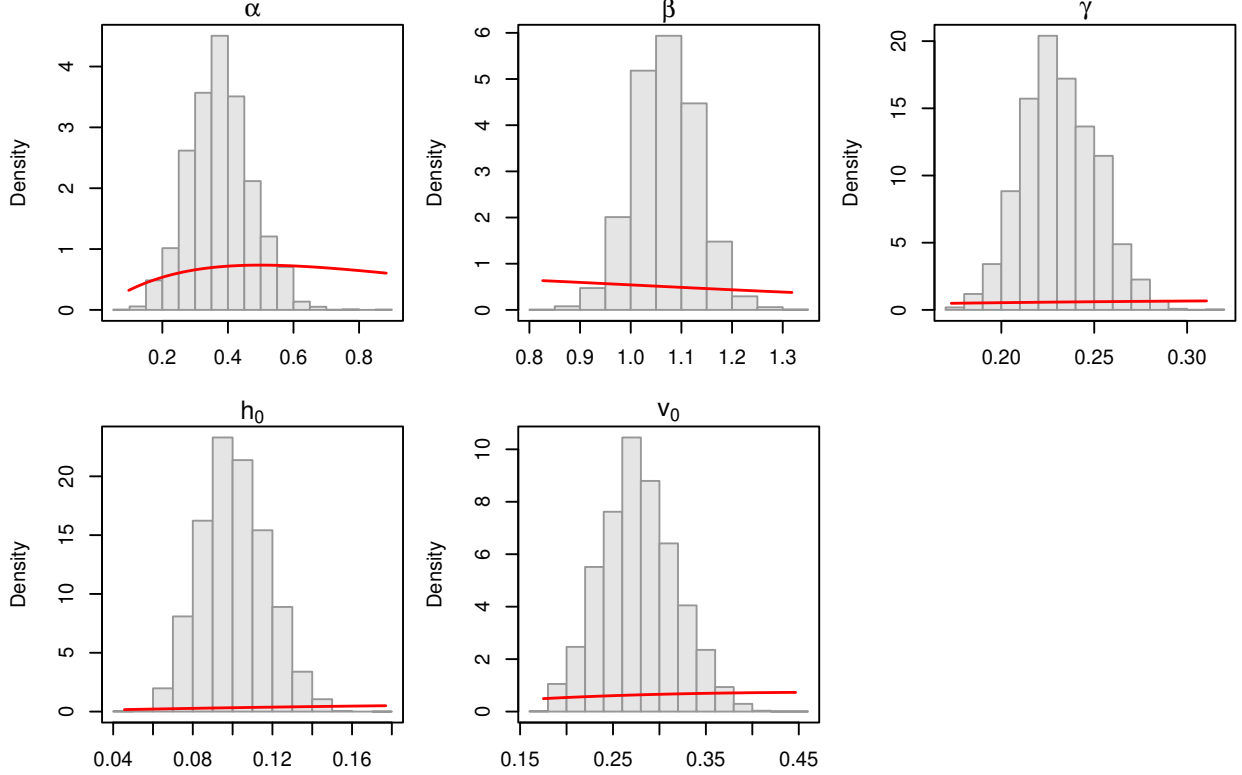


Figure 7: Posterior distributions ($n=2000$) for the underdamped hazard model parameters. The relevant part of the prior density is shown in red.

level while estimating the oscillation frequency ω directly from the data (without imposing a fixed calendar period). We analyze the intercept-only baseline to characterize the underlying hazard shape; covariates are omitted here to focus inference on the baseline dynamics.

To choose the initial parameters, we employ simple data-driven values that are consistent with the local interpretation of the model. Specifically, the initial parameter values are chosen to correspond to the survival function $S(\Delta t)$, $S(2\Delta t)$, and $S(3\Delta t)$ for a small time step Δt . Further details can be found in [9]. Following same argument, for the hazrad model in (Eq. 19), we have

$$h_0 = -\frac{S'(0)}{S(0)} = -\frac{S(\Delta t) - S(0)}{\Delta t S(0)},$$

$$h'(0) = v_0 = \frac{S'(0)^2 - S(0)S''(0)}{S(0)^2} \approx \left(\frac{S(\Delta t) - S(0)}{\Delta t S(\Delta t)} \right)^2 - \frac{S(2\Delta t) - 2S(\Delta t) + S(0)}{\Delta t^2 S(\Delta t)},$$

and

$$\omega^2 = -\frac{h''(0)}{h_0 - c}$$

$$\begin{aligned}
h''(0) &= -\frac{S'''(0)}{S(0)} + \frac{3S''(0)S'(0)}{S(0)^2} - \frac{2S'(0)^3}{S(0)^3} \\
&\approx -\frac{S(3\Delta t) - 3S(2\Delta t) + 3S(\Delta t) - S(0)}{\Delta t^3 S(\Delta t)} \\
&\quad + \frac{3[S(2\Delta t) - 2S(\Delta t) + S(0)][S(\Delta t) - S(0)]}{\Delta t^3 S(\Delta t)^2} \\
&\quad - \frac{2[S(\Delta t) - S(0)]^3}{\Delta t^3 S(\Delta t)^3}.
\end{aligned}$$

The initial baseline shift (c_0) was initialized as the average hazard over the observed window. Following our initialization scheme for ω_0 , h_0 , and v_0 , we take $\Delta t = 1/12$ (one month), set $S(0) = 1$, and estimate a near-time-zero rate

$$\hat{\lambda} = \frac{\sum_{i=1}^n \mathbf{1}\{t_i \leq \Delta t\} \delta_i}{\sum_{i=1}^n \min(t_i, \Delta t)} \quad (\text{per year}),$$

where $\delta_i = \mathbf{1}\{\text{status}_i = 2\}$. We then stabilize the forward-difference formulas by anchoring a local exponential survival curve,

$$S(\Delta t) = \exp(-\hat{\lambda} \Delta t), \quad S(2\Delta t) = \exp(-2\hat{\lambda} \Delta t), \quad S(3\Delta t) = \exp(-3\hat{\lambda} \Delta t),$$

which are plugged into the expressions for $h(0)$, $h'(0)$, and $h''(0)$ to obtain starting values ω_0 , h_0 , and v_0 for maximum likelihood estimation. When these choices are uncertain, a Bayesian approach with an informative prior centered on these values is appropriate.

We compared the sinusoidal hazard model against the standard parametric models, namely the log-normal and Weibull distributions, using the Bayesian information criterion (BIC):

$$BIC = k \log(n) - 2\ell$$

where n is the sample size, k is the number of parameters, and ℓ is the maximized log-likelihood. The BIC values were 371.38 (weibull), 402.21 (log-normal), and 384.01 (sinusoidal). Although the sinusoidal hazard model did not achieve the minimum BIC for this dataset, it provides a flexible framework for modeling survival data with seasonal or periodic effects. In particular, the sinusoidal structure allows the hazard rate to vary smoothly over time, capturing cyclical risk patterns that standard monotone or unimodal models may fail to represent.

9 Conclusion

This work advances dynamical survival analysis by introducing a class of hazard models governed by higher-order ODEs. By allowing the hazard to evolve according to both its current level and its temporal derivatives, the proposed framework substantially broadens the range of risk dynamics that can be represented within a coherent survival modeling paradigm, with direct relevance for medical and biomedical research where risk evolves over time in response to treatment, disease progression, or physiological adaptation. In particular, higher-order formulations accommodate inertia, delayed responses, and oscillatory behavior, yielding hazard trajectories and induced survival distributions that are inaccessible under conventional first-order or monotone hazard assumptions.

Through a collection of nonlinear and oscillatory examples, we demonstrate how interpretable dynamical mechanisms translate directly into flexible hazard behavior and complex time-to-event patterns. The accompanying numerical framework enables practical implementation across model

classes, supporting solution of higher-order systems, evaluation of cumulative hazards, likelihood-based inference under censoring, and simulation of event times. Together, these components establish higher-order ODE-based hazards as a viable and expressive alternative to static or memoryless survival models, particularly in applications characterized by feedback-driven or temporally adaptive risk.

Despite its flexibility, the proposed framework also has limitations. Higher-order hazard models introduce additional parameters and latent dynamics, which may complicate identifiability and increase computational cost, particularly in data-limited settings. Model specification requires careful consideration of parameter choices, dynamical structure, and time-scale normalization to ensure the existence of a positive hazard function and meaningful temporal interpretation. In particular, the inclusion of an explicit scale parameter is essential for preserving hazard shape across different time scales [9], consistent with standard parametric survival modeling practice. Inappropriate modeling choices may lead to instability or overfitting. Moreover, the present work focuses primarily on deterministic hazard dynamics, and stochastic perturbations or measurement noise are not explicitly modeled. These limitations point to promising directions for future work. A natural extension of this framework is to introduce stochastic perturbations into the hazard dynamics through stochastic differential equation formulations. Also, as a baseline for the real-life application, we use the exponential survival model with a constant hazard. This assumption can be relaxed by adopting models such as the Weibull that allow the hazard to vary over time.

Overall, higher-order dynamical hazard models offer a principled and flexible approach to capturing complex temporal risk patterns, opening new avenues for survival analysis in systems where risk evolves with memory, feedback, and adaptation.

Code Availability

The code used in this study is available upon request.

Declaration of Interests

The author has no conflicts of interest to report.

Contributions

Authors DL, MBH, and FM contributed to the formulation and analysis of the models, graphical presentations, data curation, and the simulation study; FM conceptualized and directed the research. All authors contributed to the literature search, model evaluations, and the writing of the paper.

Ethics Approval

There is no ethical approval needed due to the use of simulated and publicly available data.

Funding Statement

The authors do not have funding to report.

References

- [1] Liberato Camilleri. History of survival analysis. 2019.

[2] Nanami Taketomi, Kazuki Yamamoto, Christophe Chesneau, and Takeshi Emura. Parametric distributions for survival and reliability analyses, a review and historical sketch. *Mathematics*, 10(20):3907, 2022.

[3] Gauss M Cordeiro, Edwin MM Ortega, and Artur J Lemonte. The exponential–weibull lifetime distribution. *Journal of Statistical Computation and simulation*, 84(12):2592–2606, 2014.

[4] Christopher Cox, Haitao Chu, Michael F Schneider, and Alvaro Munoz. Parametric survival analysis and taxonomy of hazard functions for the generalized gamma distribution. *Statistics in medicine*, 26(23):4352–4374, 2007.

[5] Edward L Kaplan and Paul Meier. Nonparametric estimation from incomplete observations. *Journal of the American statistical association*, 53(282):457–481, 1958.

[6] Kateřina Janurová and Radim Briš. A nonparametric approach to medical survival data: Uncertainty in the context of risk in mortality analysis. *Reliability Engineering & System Safety*, 125:145–152, 2014.

[7] Eben Kenah. Non-parametric survival analysis of infectious disease data. *Journal of the Royal Statistical Society Series B: Statistical Methodology*, 75(2):277–303, 2013.

[8] David R Cox. Regression models and life-tables. *Journal of the Royal Statistical Society: Series B (Methodological)*, 34(2):187–202, 1972.

[9] J Andres Christen and F Javier Rubio. Dynamic survival analysis: Modelling<? pag\break?> the hazard function via ordinary<? pag\break?> differential equations. *Statistical Methods in Medical Research*, 33(10):1768–1782, 2024.

[10] Xian Liu. *Survival analysis: models and applications*. John Wiley & Sons, 2012.

[11] Weijing Tang, Kevin He, Gongjun Xu, and Ji Zhu. Survival analysis via ordinary differential equations. *Journal of the American Statistical Association*, 118(544):2406–2421, 2023.

[12] Mikhail Izrailevich Rabinovich and Dmitriy Ivanovitsj Trubetskoy. *Oscillations and waves: in linear and nonlinear systems*, volume 50. Springer Science & Business Media, 2012.

[13] Shixiao W Jiang and John Harlim. Modeling of missing dynamical systems: Deriving parametric models using a nonparametric framework. *Research in the Mathematical Sciences*, 7(3):16, 2020.

[14] Hilary I Okagbue, Pelumi E Oguntunde, Abiodun A Opanuga, and Enahoro A Owoloko. Classes of ordinary differential equations obtained for the probability functions of exponential and truncated exponential distributions. In *Proceedings of the World Congress on Engineering and Computer Science*, volume 2, 2017.

[15] Jitsuro Sugie and Masahiko Tanaka. Nonoscillation theorems for second-order linear difference equations via the riccati-type transformation. *Proceedings of the American Mathematical Society*, 145(5):2059–2073, 2017.

[16] Yehoshua Socol, Yair Y Shaki, and Ludwik Dobrzyński. Damped-oscillator model of adaptive response and its consequences. *International Journal of Low Radiation*, 11(3-4):186–206, 2020.

[17] G Richard Price and Joel T Kalb. Insights into hazard from intense impulses from a mathematical model of the ear. *The Journal of the Acoustical Society of America*, 90(1):219–227, 1991.

[18] Moshe Gitterman. *Noisy Oscillator, The: Random Mass, Frequency, Damping*. World Scientific Publishing Company, 2012.

[19] E. C. Pielou. *Mathematical Ecology*. Wiley, New York, 1977.

[20] James D Murray. *Mathematical biology: I. An introduction*, volume 17. Springer Science & Business Media, 2007.

[21] P.-F. Verhulst. Notice sur la loi que la population poursuit dans son accroissement. *Correspondance Mathématique et Physique*, 10:113–121, 1838.

[22] J. A. Christen and F. J. Rubio. On harmonic oscillator hazard functions. *Statistics and*

Probability Letters, 217:110304, 2025.

- [23] R. Rosen. Dynamical system theory in biology. *New York Academy of Sciences*, 1987.
- [24] B. Zhang and K. Gopalsamy. Periodicity in a periodic logistic equation with delay. *Journal of Mathematical Biology*, 1990.
- [25] D. Schley and S. Gourley. Stability switches in a delayed logistic equation. *Proceedings of the Royal Society A*, 2000.
- [26] Christopher Stanley, Elizabeth Molyneux, and Mavuto Mukaka. Comparison of performance of exponential, cox proportional hazards, weibull and frailty survival models for analysis of small sample size data. *Journal of Medical Statistics and Informatics*, 4(1), 2016.
- [27] Barbara Helm, Rachel Ben-Shlomo, Michael J Sheriff, Roelof A Hut, Russell Foster, Brian M Barnes, and Davide Dominoni. Annual rhythms that underlie phenology: biological time-keeping meets environmental change. *Proceedings of the Royal Society B: Biological Sciences*, 280(1765):20130016, 2013.
- [28] J Aschoff. Adaptive cycles: their significance for defining environmental hazards. *International Journal of Biometeorology*, 11:255–278, 1967.
- [29] Mahmudul B. Hridoy. An exploration of modeling approaches for capturing seasonal transmission in stochastic epidemic models. *Mathematical Biosciences and Engineering*, 22(2):324–354, 2025.
- [30] David W Zingg and Todd T Chisholm. Runge–kutta methods for linear ordinary differential equations. *Applied Numerical Mathematics*, 31(2):227–238, 1999.
- [31] Karline Soetaert, Thomas Petzoldt, and R Woodrow Setzer. Solving differential equations in r: package desolve. *Journal of statistical software*, 33:1–25, 2010.
- [32] Subhabrata Chakraborti, Felipe Jardim, and Eugenio Epprecht. Higher-order moments using the survival function: The alternative expectation formula. *The American Statistician*, 2019.
- [33] Pingfan Song, Changchun Tan, and Shaochen Wang. On the moment generating function for random vectors via inverse survival function. *Statistics & Probability Letters*, 145:345–350, 2019.

A Monotonicity and Nonmonotonicity in ODEs

For first-order ODEs, monotonicity of solutions is closely tied to the sign of the derivative along solution trajectories. Consider an autonomous first-order ODE

$$h'(t) = \psi(h(t)), \quad h(t_0) = h_0.$$

If $\psi(h(t))$ maintains a constant sign along the trajectory of the solution, then $h(t)$ is monotonic on its interval of existence. For example, when $\psi(h) = kh$ with $k > 0$, the solution $h(t) = h_0 e^{k(t-t_0)}$ is strictly increasing. Conversely, if $\psi(h(t))$ changes sign along the trajectory, the solution may exhibit nonmonotonic behavior, such as local maxima or minima, depending on the structure of ψ .

First-order ODEs have been widely used to model hazard dynamics in survival analysis, providing a unified perspective on classical models such as the proportional hazards, linear transformation, and accelerated failure time models [4, 10]. Within this framework, the evolution of the hazard is governed solely by its current level, which imposes strong structural constraints on admissible temporal behavior. In particular, first-order autonomous systems naturally favor monotonic or asymptotically monotonic hazard trajectories.

In contrast, monotonicity becomes substantially more restrictive in higher-order ODEs. For instance, consider the second-order linear ODE

$$h''(t) = -kh(t), \quad h(t_0) = h_0, \quad h'(t_0) = v_0,$$

with $k > 0$. Its solutions take the form

$$h(t) = A \cos(\sqrt{k}t) + B \sin(\sqrt{k}t),$$

which are inherently oscillatory and therefore nonmonotonic. More generally, higher-order ODEs introduce additional state variables, such as the hazard derivative, that act as latent dynamical components. Even when the system is autonomous, these hidden states permit feedback, inertia, and delayed responses, making nonmonotonic behavior generic rather than exceptional.

Nonlinear higher-order systems further expand the range of possible dynamics. For example, the nonlinear second-order equation

$$h''(t) + h(t)^3 = 0$$

admits bounded oscillatory solutions whose amplitude and frequency depend on initial conditions. Such dynamics can generate transient risk increases, cyclic hazard patterns, and delayed effects that cannot be captured within first-order formulations.

From the perspective of hazard modeling, nonmonotonic hazard functions may arise either through explicit time dependence or through higher-order dynamics that implicitly encode memory via additional state variables. Second-order and higher-order ODEs thus provide a natural mechanism for generating nonmonotone hazards without requiring nonautonomous forcing. While many commonly used hazard models can be expressed as solutions to first-order equations under specific boundary conditions such as $\lim_{t \rightarrow 0} h(t) = 0$ or ∞ , higher-order formulations substantially extend this class by enabling richer temporal behavior.

B Proof of Theorem 2

Proof. 1. Eq. 11 is a linear ODE with constant coefficients. By standard existence and uniqueness theory for linear systems, for any $h_0 > 0$ and $v_0 \in \mathbb{R}$ there is a unique solution $h(t)$ defined for all $t \geq 0$.

2. Set $h^* = \gamma/\beta$ and define $y(t) = h(t) - h^*$. Substituting gives

$$y''(t) + \alpha y'(t) + \beta y(t) = 0.$$

Its characteristic equation is $r^2 + \alpha r + \beta = 0$, with roots

$$r_{1,2} = \frac{-\alpha \pm \sqrt{\alpha^2 - 4\beta}}{2}.$$

If $\alpha > 0$ and $\beta > 0$, then $\Re(r_1), \Re(r_2) < 0$, so $y(t) \rightarrow 0$ as $t \rightarrow \infty$, hence $h(t) \rightarrow h^* = \gamma/\beta$.

3. The qualitative form follows from the roots: if $\Delta = \alpha^2 - 4\beta < 0$ the roots are complex with real part $-\alpha/2$, giving damped oscillations; if $\Delta = 0$ there is a repeated root $-\alpha/2$, giving critical damping; if $\Delta > 0$ there are two distinct negative real roots, giving an overdamped sum of decaying exponentials.

□

C Monte Carlo Simulation for Nonlinear Hazard Models

Algorithm 2 Monte Carlo Simulation for Nonlinear Hazard Models

Require: Parameter settings for each hazard model, sample sizes $n \in \{500, 1000, 2000, 5000\}$, number of replications $R = 20,000$

Ensure: Posterior summaries and RMSEs for each model and sample size

for each hazard model (Damped Oscillatory, Population Dynamics, Sinusoidal, Exponential with interaction) do

2: Set true parameter values according to model specification

for each sample size n do

4: for replication $r = 1$ to R do

Simulate n true event times $\{T_i\}_{i=1}^n$ from the model using numerical solver of second-order ODE

6: Generate n censoring times $\{C_i\}_{i=1}^n$ independently from a $\text{Uniform}(0, c_{\max})$ distribution, tuned to yield 20–30% censoring

Define observed times: $t_i = \min(T_i, C_i)$ and event indicators: $\delta_i = \mathbb{I}(T_i \leq C_i)$

8: Fit the model using Bayesian inference:

- Use weakly informative priors (e.g., $\text{Gamma}(2, 2)$ for positive parameters)
- Run t-walk MCMC sampler for 10,000 iterations
- Discard the first 10,000 iterations as burn-in
- Apply thinning (retain every 5th draw) to yield 20,000 posterior samples

Compute posterior means for model parameters

10: end for

Compute root mean squared error (RMSE) and posterior summary statistics (e.g., mean, SD) across the R replications

12: end for

end for

14: return Posterior means, standard deviations, and RMSEs for each model and sample size

D Additional Simulation Results

D.1 Damped hazard model

Table 2: Posterior results for the critically damped hazard model. True parameter values are shown in parentheses.

		α (2)	γ (0.2)	h_0 (0.1)	v_0 (0.3)
$n = 200$	Mean	2.9992	0.5213	0.1679	0.2120
	RMSE	1.3782	0.4591	0.0820	0.1901
$n = 500$	Mean	2.5740	0.3945	0.1572	0.2391
	RMSE	1.0176	0.3341	0.0672	0.1532
$n = 1000$	Mean	2.5427	0.3817	0.1258	0.2625
	RMSE	0.9691	0.3151	0.0388	0.1186
$n = 2000$	Mean	2.4550	0.3380	0.1081	0.2940
	RMSE	0.7853	0.2500	0.0216	0.0881
$n = 5000$	Mean	1.9391	0.2017	0.1004	0.2803
	RMSE	0.4382	0.1110	0.0129	0.0635

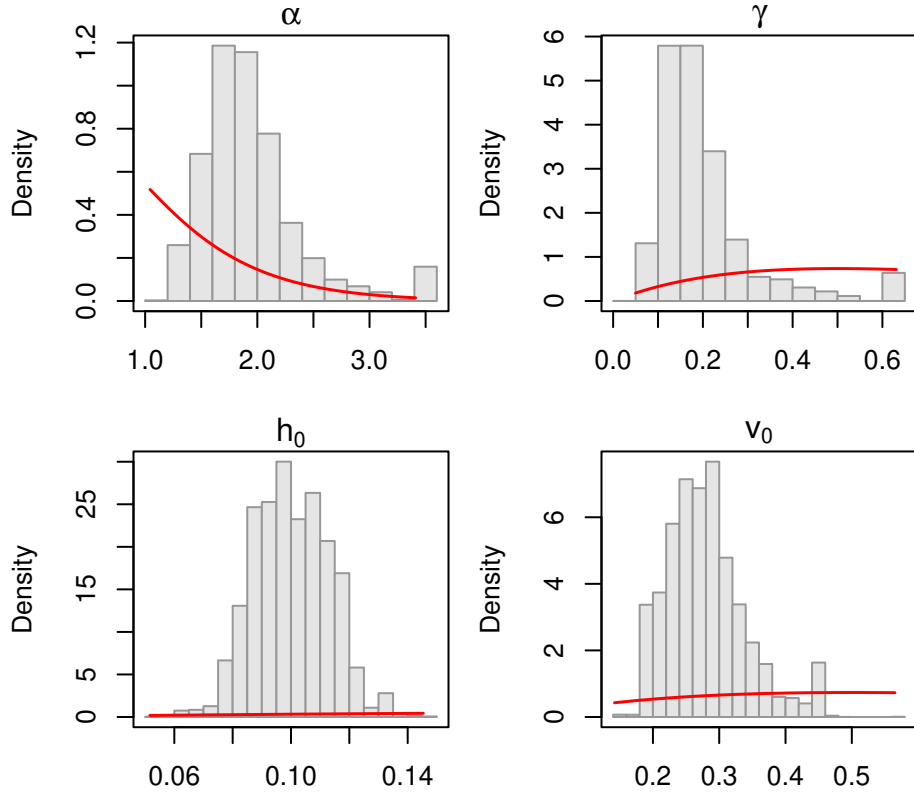


Figure 8: Posterior distributions ($n=2000$) for the critically damped hazard model parameters. The relevant part of the prior density is shown in red.

Table 3: Posterior results for the overdamped hazard model. True parameter values are shown in parentheses.

		α (3)	β (1)	γ (0.2)	h_0 (0.1)	v_0 (0.3)
$n = 200$	Mean	2.8125	1.1434	0.2326	0.0973	0.4313
	RMSE	0.8777	0.6084	0.1412	0.0519	0.2473
$n = 500$	Mean	2.7514	1.0504	0.2227	0.0842	0.2957
	RMSE	0.8793	0.6268	0.1408	0.0358	0.1350
$n = 1000$	Mean	2.9015	1.1208	0.2300	0.1024	0.2358
	RMSE	0.8047	0.6487	0.1330	0.0265	0.1349
$n = 2000$	Mean	2.8021	1.1172	0.2437	0.0985	0.2821
	RMSE	0.7568	0.6898	0.1572	0.0204	0.1029
$n = 5000$	Mean	2.4024	0.8495	0.1689	0.1034	0.2429
	RMSE	0.8751	0.5269	0.1115	0.0145	0.0987

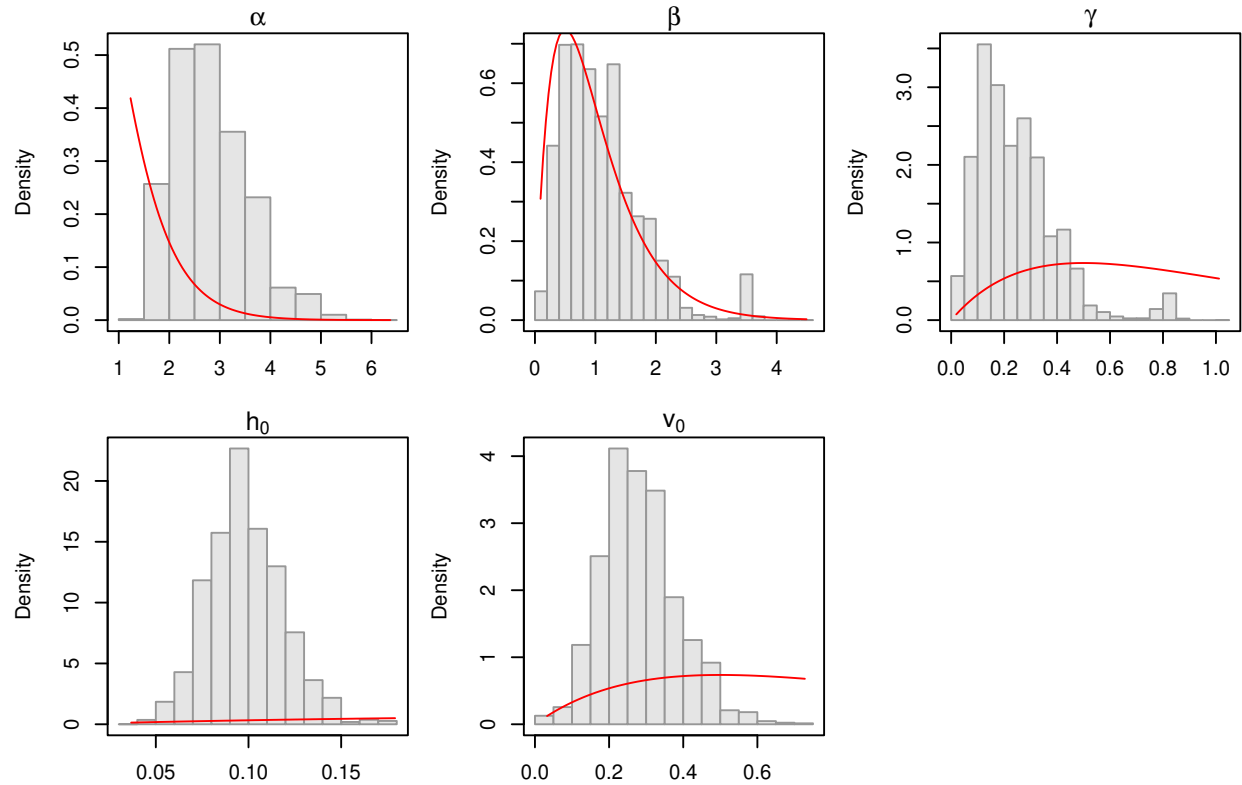


Figure 9: Posterior distributions ($n=2000$) for the overdamped hazard model parameters. The relevant part of the prior density is shown in red.

D.2 Population dynamics-based hazard model

Table 4: Posterior results for the population dynamics-based hazard model. True parameter values are shown in parentheses.

		$r(0.8)$	$\zeta(0.5)$	$K(1)$	$h_0(0.1)$	$v_0(0.2)$
$n = 200$	Mean	0.9774	0.9994	1.0240	0.0818	0.3728
	RMSE	0.7063	0.7218	0.4495	0.0452	0.2253
$n = 500$	Mean	1.2490	0.7449	1.0382	0.0862	0.2479
	RMSE	0.9390	0.4499	0.4030	0.0315	0.1072
$n = 1000$	Mean	1.2368	0.7126	0.9353	0.1046	0.1912
	RMSE	0.9311	0.4260	0.2457	0.0231	0.0642
$n = 2000$	Mean	1.2947	0.7034	1.0430	0.0965	0.2201
	RMSE	0.9837	0.4189	0.1800	0.0175	0.0557
$n = 5000$	Mean	1.0432	0.6564	0.9987	0.0950	0.2196
	RMSE	0.7000	0.3434	0.1185	0.0125	0.0386

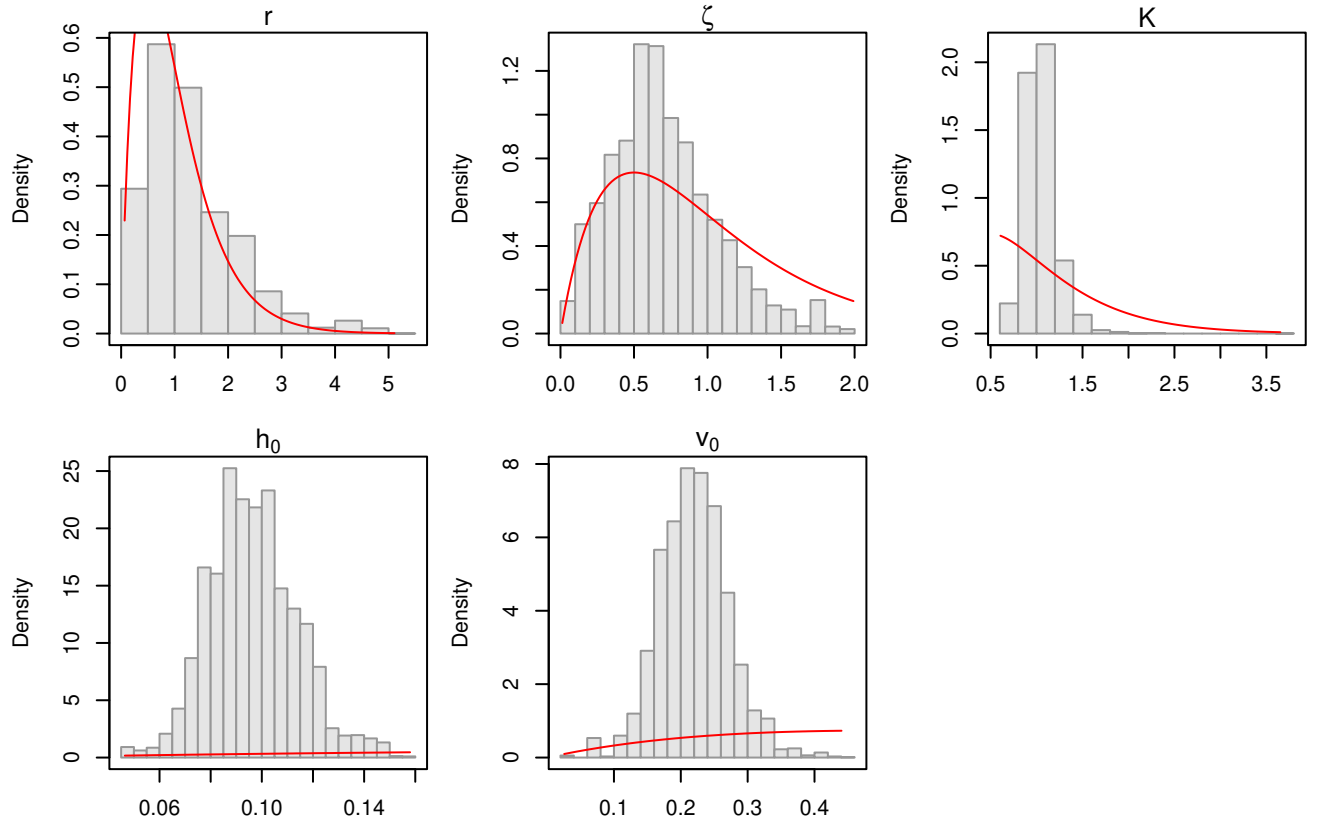


Figure 10: Posterior distributions ($n=2000$) for the population dynamics-based hazard model. The relevant part of the prior density is shown in red.

D.3 Sinusoidal hazard model

Table 5: Posterior results for the sinusoidal hazard model. True parameter values are shown in parentheses.

		ω (0.2π)	c (0.6)	h_0 (0.1)	v_0 (0.2)
$n = 200$	Mean	0.7396	0.6326	0.1387	0.1641
	RMSE	0.1915	0.1444	0.0554	0.0608
$n = 500$	Mean	0.7568	0.5714	0.1028	0.1609
	RMSE	0.1565	0.0646	0.0230	0.0558
$n = 1000$	Mean	0.6928	0.6216	0.1048	0.1497
	RMSE	0.1114	0.0928	0.0184	0.0614
$n = 2000$	Mean	0.6723	0.6448	0.1056	0.1817
	RMSE	0.0741	0.0659	0.0140	0.0311
$n = 5000$	Mean	0.6432	0.6347	0.1035	0.1820
	RMSE	0.0396	0.0471	0.0092	0.0257

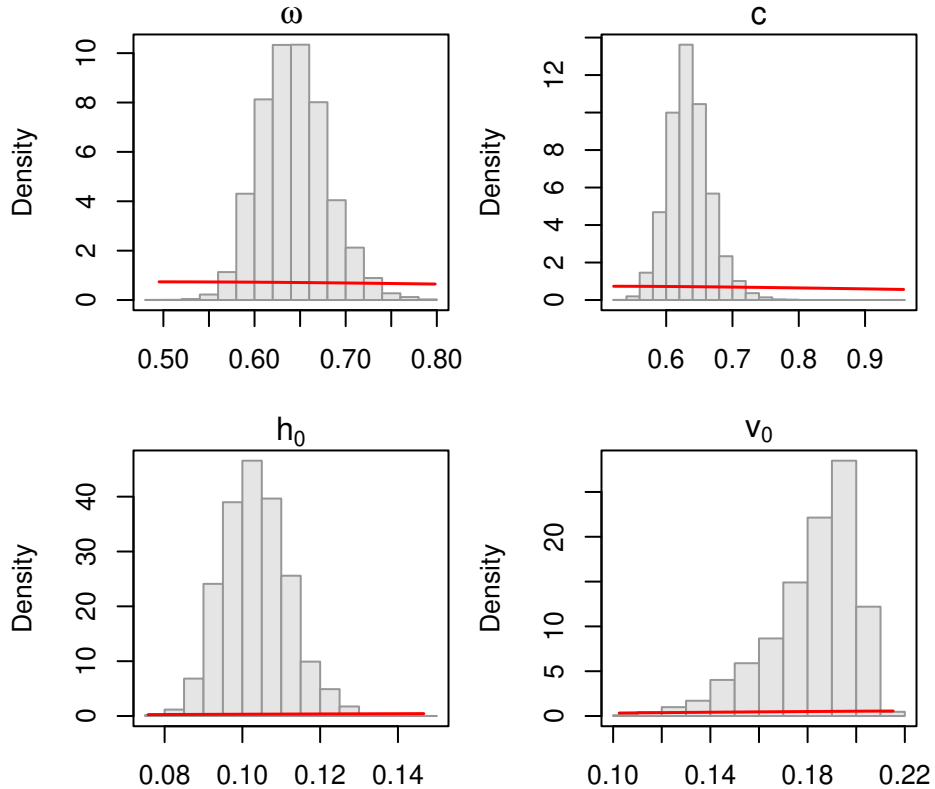


Figure 11: Posterior distributions ($n=2000$) for the sinusoidal hazard model parameters. The relevant part of the prior density is shown in red.

D.4 Exponential hazard model with interaction effects

Table 6: Posterior results for the exponential hazard model (when $\beta = 0$). True parameter values are shown in parentheses.

		α (0.1)	h_0 (0.4)	v_0 (0.1)
$n = 200$	Mean	0.1399	0.4415	0.0794
	RMSE	0.0693	0.0683	0.0387
$n = 500$	Mean	0.1185	0.3873	0.0862
	RMSE	0.0399	0.0361	0.0268
$n = 1000$	Mean	0.1186	0.3874	0.0941
	RMSE	0.0369	0.0283	0.0214
$n = 2000$	Mean	0.1358	0.3952	0.1023
	RMSE	0.0456	0.0199	0.0200
$n = 5000$	Mean	0.1056	0.3919	0.0980
	RMSE	0.0174	0.0148	0.0136

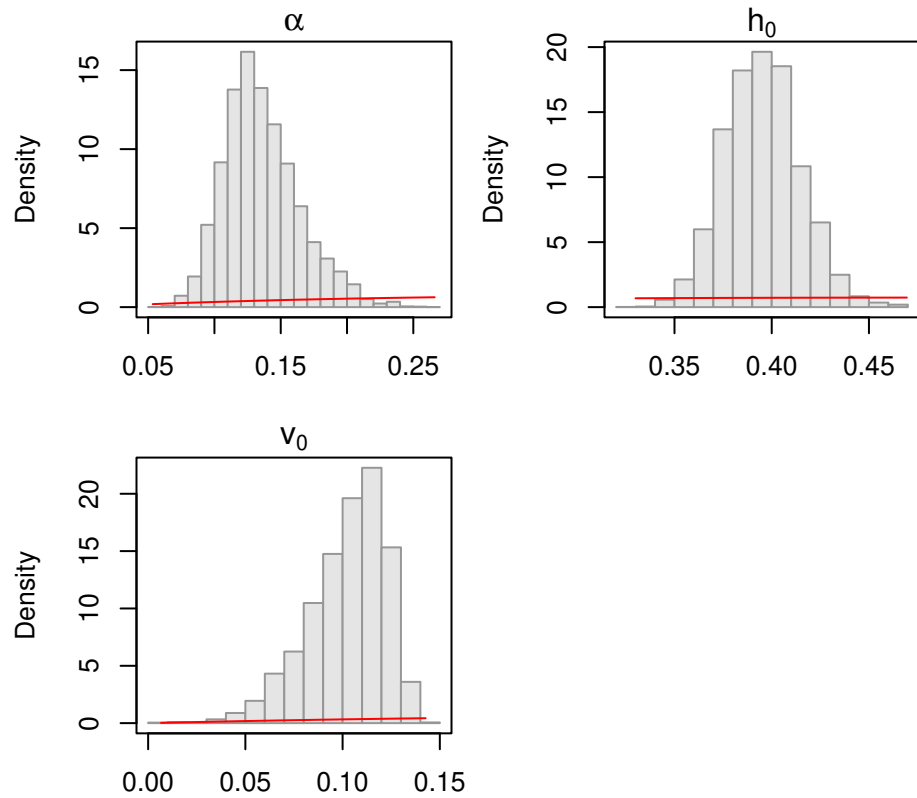


Figure 12: Posterior distributions ($n=2000$) for the exponential hazard model parameters (when $\beta = 0$). The relevant part of the prior density is shown in red.